Segmentation of Synapses in Fluorescent Images using U-Net++ and Gabor-based Anisotropic Diffusion

Yan, Yifei; Qiu, Zhen; Zhang, Qi

Published in:
ICMIPE 2021 Conference Proceedings

DOI:
10.1109/ICMIPE53131.2021.9698901

Publication date:
2021

Document Version
Peer reviewed version

Segmentation of Synapses in Fluorescent Images using U-Net++ and Gabor-based Anisotropic Diffusion

Yifei Yan[1,2], Zhen Qiu[3], Qi Zhang[1,2] *

[1]Shanghai Institute for Advanced Communication and Data Science, The SMART (Smart Medicine and AI-based Radiology Technology) Lab, Shanghai University, Shanghai, China

[2]School of Communication and Information Engineering, Shanghai University, Shanghai, China

[3]Centre for Clinical Brain Sciences, University of Edinburgh, Edinburgh, UK

*Corresponding author: Qi Zhang (zhangq@t.shu.edu.cn)

***Abstract*—**Objective: Automation of efficient and reliable synapse detection and quantification in fluorescent images is essential for the high-throughput investigation of synaptic features. However, the automatic segmentation of synapses is susceptible to interference from non-synaptic tissue and multiplicative Poisson noise. Therefore, a time-saving and labor-saving automatic synaptic segmentation framework is necessary. Methods: we proposed an automatic synapse segmentation framework using a deep learning method based on a modified U-Net++ and Gabor-based anisotropic diffusion (GAD). The modified U-Net++ was used to segment the non-synaptic region, while the multiplicative Poisson noise was suppressed and the edge of the synapse was enhanced by the GAD filter. Thereafter, the synapses were segmented by a thresholding method. Results: The non-synaptic regions were segmented precisely, and its Dice coefficient and Jaccard similarity were 0.833 and 0.719. Our model for synapse segmentation reduced the interference from the non-synaptic tissues and Poisson noise and yielded automatic and accurate segmentation of synapses. Conclusion: We have proposed an automatic segmentation framework that can accurately segment non-synaptic and synaptic tissues, which may have the potential to automate the quantitative analysis of synapses.

Keywords: synapse, image segmentation, Gabor-based anisotropic diffusion, U-Net++

I. Introduction

As the fundamental sites of electrochemical signal transmission within the brain, neuronal synapses transmit nerve impulses from one neuron to another neuron or a non-neuronal cell [1], which is the basis of human perception, learning, memory and cognition[2]. Among them, the scaffold protein PSD95 in the composition of pre-synaptic and post-synaptic density proteins is one of the most abundant proteins in the brain and plays a key role in many innate and acquired behaviors[3-5]. Therefore, the study of synapses expressing PSD95 is extremely important. However, due to the high spatial density and structural complexity of synapses, new computational tools are required to effectively identify PSD95-positive synapses[6].

Fluorescence microscopy (FM) can completely obtain high-throughput images of the molecular-level large field of view of the slices, and the PSD95-positive synapses in the image can be identified as spots combined with immunostaining technology[7]. However, compared with other animals, the non-synaptic structures such as blood vessels and nerve cell bodies of the human brain are more complicated, which brings great interference to the detection of synapses in FM images. At the same time, FM images are usually polluted by Poisson-distributed multiplicative noise and with small signal to noise ratio(SNR)[8]. However, reliable and efficient synapse detection is the key to high-throughput research on synaptic characteristics. Therefore, how to detect and segment synapses quickly and accurately under the background of non-synaptic tissue and noise interference is an important challenge for subsequent quantitative analysis of synapses.

The common practice of synaptic quantization is still largely manual or semi-manual. In recent years, computer vision technology has been used to automate synaptic detection. In [9], the edge of the synaptic point is obtained by detecting the gray gradient between the synaptic point and the adjacent region. In addition, support vector machine (SVM) is used in [10] to estimate the confidence of the synapse of a pixel as an adjacent pixel, then evaluate the local confidence and compare it with the minimum confidence, and then detect the synapse according to these confidence values.

The above methods based on machine learning are easily disturbed by non-synaptic tissue and multiplicative Poisson noise in the process of synapse segmentation. Here, we propose an automatic synapse segmentation framework based on deep learning and GAD filtering, which can suppress the interference of non-synaptic regions and noise and segment synapses accurately and quickly.

II. Materials and Methods

A. Image Acquisition

Post-mortem human brain tissue was obtained from the Medical Research Council UK (MRC) funded University of

Edinburgh Brain Bank (EBB). All procedures involving post-mortem human brain tissue were approved by the East of Scotland Research Ethics Service (16/ES/0084). Informed written consent was obtained concerning each subject.

The tissue sections were from the hippocampal area of three human brains with normal phenotypes. During the autopsy, according to EBB protocol, the brain tissue was dissected into 1mm thick tissue sections, which were scanned by fluorescent microscope Nikon Ti2 microscope and labeled with PSD95-positive Synapses.

For the visualization of the whole-mounted brain sections, the size of the image after cutting is 958 × 940 pixels, pixel resolution was 0.07 × 0.07 μm, and image brightness was in a depth of 16 bits. 600 images were selected from all slices with labeled non-synaptic tissues as a dataset for subsequent experiments, 500 of them were used as training sets and 100 as test sets. Figure 1 shows a typical example of fluorescent image and its corresponding labeling of non-synaptic tissues namely vessels and nerve cell bodies.

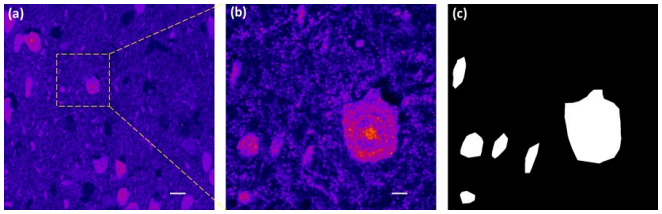

Fig. 1. An example of the image in our dataset (a): Large scale FM image (b): Input image to the network (c): Binary mask of Non-synaptic tissue. The scale bar on the large scale image equals 20μm(5μm in the cropped image)

B. *Overview of the Automatic Segmentation framework*

In this work, we put forward a synapse FM image segmentation method, including the following three steps. Firstly, a modified U-Net ++ neural network is used to segment the non-synaptic tissues in FM images. Then, the GAD filter was used to filter out speckle noise and enhance synapse edge, followed by thresholding the GAD-filtered image to finally segment the synapses.

C. *U-Net++-based Segmentation of non-synaptic tissues*

Since the size of typical mammalian synapses is close to the diffraction limit of light, individual synapses are decomposed into spots in FM images[6]. Direct segmentation of synapses using deep learning methods depends on the pre-labeling of synapses[11]. Synaptic labeling is extremely time-consuming and labor-intensive due to the enormous quantity. Therefore, the modified U-Net ++ network was used to segment the non-synaptic tissues.

The structure of the modified U-Net++ is shown in Figure 2. U-Net++ starts with an encoder sub-network or backbone followed by a decoder sub-network[12]. What distinguishes U-Net++ from U-Net is the re-designed skip pathways[13]. In U-Net, the feature maps of the encoder are directly received in the decoder, in U-Net++, they undergo a dense convolution block whose number of convolution layers depends on the pyramid level. In addition, the scheme of deep supervision is mentioned, which gives us the direction of improvement.

Considering the segmentation of non-synaptic tissues is mainly based on the size and gray gradient, the overall task is not complicated. The deeper network is easier to overfit and with more parameters. Therefore, we prune the 4-layer U-Net ++ network to 3-layer. In addition, considering that the gray gradient between non-synaptic tissues and synapse is similar but significantly different in size, we modified the pooling operation of the downsampling layer. Firstly, the receptive fields of all pooling layers were expanded from 2 × 2 to 3 × 3, allows for non-synaptic tissue edges more accurately located during downsampling between $C^{i,0}$ to $C^{i+1,0}$,$i \in \{0,1,2\}$, Where $C^{i,0}$ represents the i-th input convolution block. Then, the original Maxpooling layers of $C^{1,0}$-$C^{2,0}$, and $C^{2,0}$-$C^{3,0}$ were changed to Avgpooling. This step can inhibit the segmentation of uncertain regions such as big synapses based on the advanced features (texture, morphology) extracted after the first down-sampling.

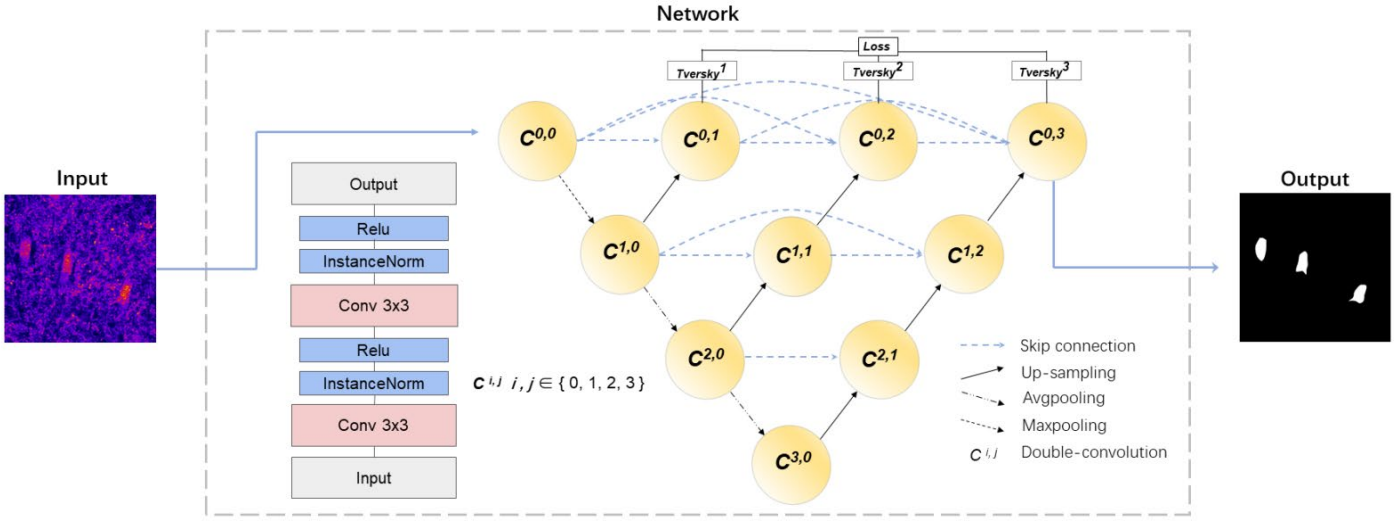

Fig. 2. The segmentation scheme based on the modified U-Net++ for non-synaptic tissues

In the training process of the model, Tversky loss was used as the loss function for the output of each layer [14]; For each given pixel, the Tversky was defined as:

$$Tversky(\alpha,\beta)=\frac{\sum_{N}^{i=1} p_{0i}g_{0i}}{\sum_{N}^{i=1} p_{0i}g_{0i}+\alpha\sum_{N}^{i=1} p_{0i}g_{1i}+\beta\sum_{N}^{i=1} p_{1i}g_{0i}} \tag{1}$$

Where in the output of the sigmoid layer, the p^{0i} is the probability of pixel i be a lesion and p^{1i} is the probability of pixel i be a non-lesion, g^{0i} is 1for a lesion pixel, and 0 for a non-lesion pixel for the g^{1i}. where α and β control the magnitude of penalties for FPs(false positive) and FNs(false negative), respectively. For α and β, we take 0.3 and 0.7 respectively. Assume Tversky ^{j}, $j \in \{1,2,3\}$ is used to represent the Loss function of $C^{0,\ j}$, $j \in \{1,2,3\}$ layer. Therefore, the average loss function of the three output layers is used as the loss function.

$$Loss=\sum_{j=1}^{3} Tversky^{j}/3 \quad j\in\{1,\ 2,\ 3\} \tag{2}$$

All the training and evaluation were performed on a desktop computer with a 64-Linux system with GTX 1080ti GPU with 11 GB RAM based on PyTorch. The learning rate was initially set to 2.5e-3, with momentum 0.9 and weight decay 0.001. The model was trained for 50 epochs with batch size 2 and stochastic gradient descent. Data augmentation methods were applied to increase the training data size, including flipped horizontally, rotated randomly between [−5◦, 5◦], and transformation of brightness and contrast.

D. GAD based synapse edge enhancement and Threshold segmentation

In this section, we introduce the GAD to suppress speckle noise and enhance synapse edges. Then the synapse is segmented by the threshold method.

The GAD is a speckle reduction method by employing an edge detector based on the Gabor transform into the anisotropic diffusion [15]. We can use the formulation $I(x, y)$*imag[$g_d(x, y)$] to denote the Gabor transform $G_d(x, y)$, Where, an input image is denoted as $I(x, y)$, * represents the convolution operator, imag[·] denotes the imaginary part, and G_d (x, y) is the d-th convoluted image obtained by convolving the d-th Gabor kernel $g_d(x, y)$ with the input image. Here, only the imaginary part of the Gabor kernel is utilized for convolution [15]. Edge detector based on the Gabor is hence given by:

$$G_{\mathrm{sd}}(x,y)=\sqrt{\frac{1}{D-1}\sum_{d=0}^{D\text{-}1}[G_d(x,y)]^2} \tag{3}$$

The GAD model can be described by the following partial differential equation:

$$\begin{cases}\dfrac{\partial I(x,y)}{\partial t}=\mathrm{div}[c(G_{\mathrm{sd}})\cdot\nabla I(x,y)]\\ I(x,y;t=0)=I_0(x,y)\end{cases} \tag{4}$$

where ∇ represents the gradient operator, div is the divergence operator, $c(\cdot)$ is the diffusion coefficient, t is the diffusion time, and I_0 is the initial image.

Concerning the GAD filtered image, we extracted the coordinates of the non-synaptic tissue, set the pixel value of the corresponding region to zero, and then emperically selected the threshold of 410, all pixels below the threshold were set to zero while the pixels above it were set to one. Finally, a binary image of the synapse is obtained.

III. EXPERIMENTAL RESULTS

A. *Quantitative evaluation of non-synaptic segmentation*

We used the Dice coefficient (DC) and Jaccard similarity (JS) to measure the performance of non-synaptic tissues segmentation. The DC and JS are expressed as:

$$\begin{cases}DC=\dfrac{2TP}{2TP+FP+FN}\\ JS=\dfrac{TP}{TP+FP+FN}\end{cases} \tag{5}$$

where TP, TN, FP, and FN denoted the numbers of true positives, true negatives, false positives, and false negatives, respectively. These evaluation metrics evaluated comprehensively the segmentation performance from different aspects. All of them were values between 0 and 1.

B. *Comparison of non-synaptic tissues segmentation results*

Figure 3 shows an example of non-synaptic tissues segmentation on an independent test set using three contrast algorithms and the modified U-Net++.

Table 1 shows the mean and standard deviation of DC and JS of several networks in independent test sets. Among them, U-Net, ResU-Net, and AttU-Net were close in results, while the average DC and JS of modified U-Net ++ reached 0.833 and 0.719 respectively. Compared with the other algorithms, the result was significantly modified.

TABLE I. PERFORMANCE COMPARISON BETWEEN THE MODIFIED U-NET++ AND U-NET, RESU-NET, ATTU-NET ON TESTING DATASET.

Model	DC	JS
U-Net	0.796±0.10	0.672±0.13
ResU-Net	0.804±0.08	0.679±0.11
AttU-Net	0.805±0.07	0.680±0.10
U-Net++	0.833±0.07	0.719±0.10

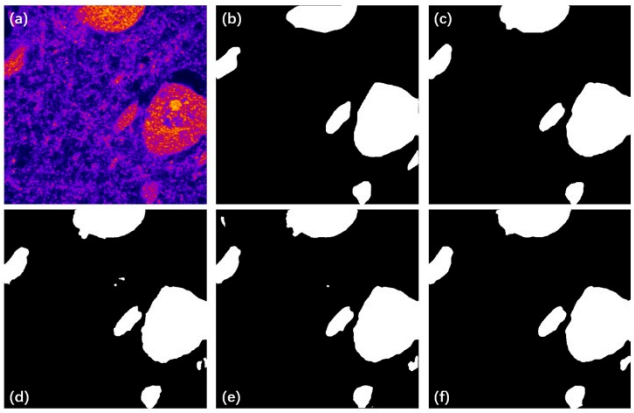

Fig. 3. Qualitative comparison of different approaches by visualization (a)original image (b) Ground truth (c) U-Net (d) ResU-Net (e) AttU-Net (f) modified U-Net ++

C. *Results of the final segmentation of synapses*

Figure 4 shows the example of synapse segmentation result using different approaches: threshold segmentation directly and the whole process proposed in this paper. It can be seen from Figure 4, the proposed automatic segmentation framework not only avoids the interference of non-synaptic tissues but also inhibits Poisson noise to achieve synapses. In contrast, the result of direct segmentation not only incorporates non-synaptic tissue into the segmentation result but also divides some larger granular noises as synapses.

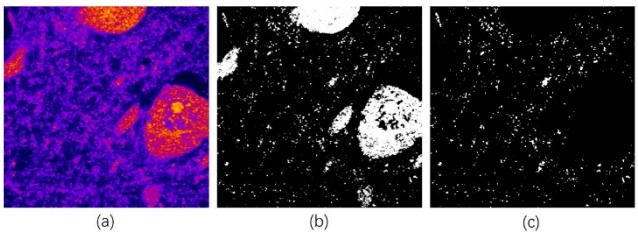

Figure4. The example using different approaches :(a) original image (b) threshold segmentation directly (c) segmented by the proposed automatic segmentation framework

IV. DISCUSSION

A synapse segmentation framework based on improved U-Net++ model combined with GAD filtering is proposed. First, the improved U-Net++ network was used to segment the non-synaptic tissue in the FM images, and then the FM images were filtered by GAD to suppress Poisson noise and enhance synaptic edges. Finally, the threshold method was used to segment the synapses. Experimental results show that the framework can accurately segment synapses in FM images and avoid interference from multiplicative Poisson noise and non-synaptic tissues (blood vessels and nerve cell bodies).

The two-stage synapse segmentation framework proposed in this work combines deep learning with traditional image processing methods to achieve precise synapse segmentation. One of the main challenges of deep learning in medical image analysis is the limited number of images and tedious annotation work. In this work, geometric and intensity transformation enhancement methods are used to amplify the data, and the labeling workload is reduced by change the labeled objects, and we also have modified the classic network U-Net++ to fit our data set. The filtering method of GAD is also used to suppress Poisson noise and solve the problem of noise masquerading as small synapses.

Although our method has obtained promising results, it also has some shortcomings and future directions. Our deep learning model still relies on fully supervised fine labeling. Therefore, we expect the methods of semi-supervised or weakly supervised can be used in the to further reduce the workload of labeling. In addition, GAD denoising and threshold segmentation will also consume additional labor. Therefore, it is expected that an end-to-end model combining these three steps will be developed.

V. CONCLUSIONS

In this study, we propose an automatic synapse segmentation framework based on a modified U-Net ++ model and GAD-based threshold segmentation. Firstly, the modified U-Net++ model was used to segment non-synaptic tissues in FM images, and the segmentation DC and JS reached 0.833 and 0.719 respectively. Then GAD was used to filter Poisson noise in FM images and enhance synaptic edges. Finally, synapses were obtained by threshold segmentation. The results in Figure 4 show that this method can effectively segment synapses. Our framework has the potential to greatly reduce the previous workload in analyzing synapses.

VI. ACKNOWLEDGMENT

The work was supported by the National Natural Science Foundation of China under Grants 61911530249 and 62071285, and Scotland XXX.

VII. REFERENCES

[1] V. K. Id, S. Guo, M. Stone, *et al.*, "DoGNet : A deep architecture for synapse detection in multiplexed fluorescence images," pp. 1–20, 2019.

[2] T. Yagi and M. Takeichi, "Cadherin superfamily genes: Functions, genomic organization, and neurologic diversity," *Genes Dev.*, vol. 14, no. 10, pp. 1169–1180, 2000.

[3] R. A. Frank and S. G. Grant, "Supramolecular organization of NMDA receptors and the postsynaptic density," *Curr. Opin. Neurobiol.*, vol. 45, pp. 139–147, 2017.

[4] R. A. W. Frank, F. Zhu, N. H. Komiyama, and S. G. N. Grant, "Hierarchical organization and genetically separable subfamilies of PSD95 postsynaptic supercomplexes," *J. Neurochem.*, vol. 142, no. 4, pp. 504–511, 2017.

[5] O. E. Curran, Z. Qiu, C. Smith, and S. G. N. Grant, "A single-synapse resolution survey of PSD95-positive synapses in twenty human brain regions.," *Eur. J. Neurosci.*, 2020.

[6] A. Kreshuk, C. N. Straehle, C. Sommer, *et al.*, "Automated Detection and Segmentation of Synaptic Contacts in Nearly Isotropic Serial Electron Microscopy Images," *PLoS One*, vol. 6, 2011.

[7] K. D. Micheva and S. J. Smith, “Array Tomography: A New Tool for Imaging the Molecular Architecture and Ultrastructure of Neural Circuits,” *Neuron*, vol. 55, 2007.

[8] I. C. Rodrigues, J. Xavier, and J. M. R. Sanches, “Fluorescence Confocal Microscopy Imaging denoising with photobleaching,” *2008 30th Annu. Int. Conf. IEEE Eng. Med. Biol. Soc.*, pp. 2205–2208, 2008.

[9] S.-M. Guo, R. Veneziano, S. Gordonov, *et al.*, “Multiplexed confocal and super-resolution fluorescence imaging of cytoskeletal and neuronal synapse proteins,” *bioRxiv*, 2017.

[10] J. Herold, M. Friedenberger, M. Bode, *et al.*, “Flexible synapse detection in fluorescence micrographs by modeling human expert grading,” pp. 1347–1350, 2008.

[11] B. Zhang, J. Zerubia, and J. Olivo-Marin, “Gaussian approximations of fluorescence microscope point-spread function models.,” *Appl. Opt.*, vol. 46 10, pp. 1819–1829, 2007.

[12] Z. Zhou, M. M. Rahman Siddiquee, N. Tajbakhsh, and J. Liang, “UNet++: A Nested U-Net Architecture for Medical Image Segmentation BT - Deep Learning in Medical Image Analysis and Multimodal Learning for Clinical Decision Support,” vol. 11045, no. 2018, pp. 3–11, 2018.

[13] O. Ronneberger, P. Fischer, and T. Brox, “U-Net: Convolutional Networks for Biomedical Image Segmentation,” *ArXiv*, vol. abs/1505.0, 2015.

[14] D. Cheng and M. Liu, “Triple crossing,” vol. 10541, no. November, pp. 106–113, 2017.

[15] Q. Zhang, H. Han, C. Ji, *et al.*, “Gabor-based anisotropic diffusion for speckle noise reduction in medical ultrasonography,” vol. 31, no. 6, pp. 1273–1283, 2014.